



## Preparation of Zinc Oxide/Graphite Composite Using Solid-State Method as an Anode Material for Lithium-Ion Battery

Hendri Widiyandari <sup>a,b,\*</sup>, Hanaiyah Parasdila <sup>a</sup>, Anisa Surya Wijareni <sup>c</sup>

<sup>a</sup> Department of Physics, Faculty of Sciences and Mathematics, Sebelas Maret University, Surakarta 57146, Indonesia

<sup>b</sup> Centre of Excellence for Electrical Energy Storage Technology, Sebelas Maret University, Surakarta 57146, Indonesia

<sup>c</sup> Department of Metallurgical Engineering, Faculty of Mining and Petroleum Engineering, Bandung Institute of Technology, Bandung, Indonesia

\*Corresponding author: [hendriwidiyandari@staff.uns.ac.id](mailto:hendriwidiyandari@staff.uns.ac.id)

<https://doi.org/10.14710/jksa.25.7.245-252>

### Article Info

#### Article history:

Received: 18<sup>th</sup> May 2022

Revised: 22<sup>nd</sup> July 2022

Accepted: 2<sup>nd</sup> August 2022

Online: 31<sup>st</sup> August 2022

#### Keywords:

Zinc oxide; Graphite; solid-state method; anode; lithium-ion battery

### Abstract

Lithium-ion batteries using zinc oxide (ZnO) as anode material had a high theoretical capacity of about 987 mAh/g. Unfortunately, ZnO capacity can drop below 200 mAh/g after only a few cycles. For that reason, graphite was added in this study due to its stable theoretical capacity of around 348–374 mAh/g to maintain the stability of lithium-ion battery capacity. Zinc oxide/graphite (ZnO/Graphite) was prepared using a solid-state method, in which ZnO and graphite were mortared until homogeneous with the mass ratio of (2:1), (1:1), and (1:2). The SEM images of all samples showed the agglomerate morphology between ZnO and graphite which affect the results of the battery performance test. The final result of the ZnO/Graphite anode can be considered a continuous anode material due to the stable cycle performance obtained in the range of 219.72–371.27 mAh/g with a decreased value of 40% after 55 cycles.

## 1. Introduction

Lithium-ion batteries are energy storage in great demand nowadays because of their outstanding performance, high power density, high energy, and long cycle life. Therefore, this is the key to the rapid development and improvement of portable electronic devices and their applications on a large scale [1]. The performance of lithium-ion batteries is highly dependent on the active materials used in the anode and cathode of lithium-ion batteries. Since the anode determines the lithium-ion battery's output voltage range [2], it is essential to research and modify the active materials used in anodes for lithium-ion batteries as they will eventually be employed in high-power applications such as electric vehicles.

The active materials that are in great demand for use as anodes in lithium-ion batteries are metal oxides. This is because the metal oxide employed will experience a redox reaction during the charge-discharge process [3]. In addition, metal oxides have prominent advantages compared to conventional carbon materials, such as high theoretical capacity, good safety performance, and wide

availability [4]. Metal oxides that have been studied in previous studies were Fe<sub>2</sub>O<sub>3</sub> [5, 6, 7] and CuO [8, 9, 10, 11].

The metal oxide that will be used is ZnO with a graphite composite since it has various advantages such as easy preparation, strong chemical stability, and inexpensive cost [12]. In addition, ZnO itself has a high theoretical capacity of 987 mAh/g [13, 14, 15, 16]. However, the zinc oxide capacity can only drop below 200 mAh/g after a few cycles [17]. For this reason, graphite composites are used because it has a stable theoretical capacity in the range of 348–374 mAh/g [18, 19]. This is expected to maintain the stability of cycle performance of ZnO for lithium-ion batteries.

The sample in this study was prepared using ZnO and graphite commercial, in which the mixing was conducted using a simple solid-state method. The solid-state method is one of the most commonly used for lithium-ion batteries because of its cost-effectiveness and ease of synthesis [20]. Therefore, this present study aimed to synthesize ZnO/Graphite as the anode for lithium-ion batteries using the solid-state method.

## 2. Methodology

### 2.1. Materials

The active ingredients used as anodes for lithium-ion batteries were zinc oxide (ZnO) (Loba Chemie, 99%) and graphite (Graphite, 99%) without further purification. The active ingredient used as the cathode for the lithium-ion battery was technical NMC-811 (Nickel Manganese Cobalt-811), produced by the Centre of Excellence for Electrical Energy Storage Technology, Sebelas Maret University.

### 2.2. Sample Preparation of Zinc Oxide/Graphite (ZnO/Graphite)

This research consisted of three main stages of work procedures: material synthesis, battery assembly, and battery performance test, as shown in the flow chart in Figure 1. The material synthesis stage involved making ZnO/Graphite composites as the battery anode using the solid-state method. In the battery assembly stage, ZnO/Graphite that had passed sample characterization were assembled to become lithium-ion batteries. The battery performance test was the stage to determine the performance of the lithium-ion batteries that have been made.

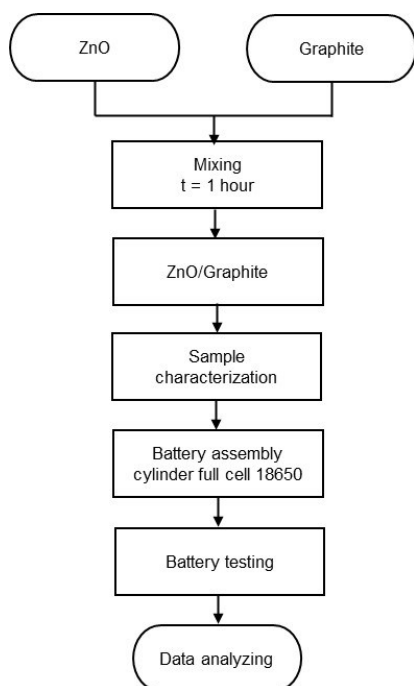


Figure 1. Research Flow of ZnO/Graphite anode

ZnO/Graphite was prepared using the simple solid-state method by varying the graphite and ZnO mass ratio. This process was started by mixing ZnO powder and graphite powder with different mass ratios, as shown in Table 1. The sample was ground using a mortar for  $\pm 1$  hour to obtain a homogeneous sample. The resulting ZnO/Graphite were then characterized. Samples that pass the characterization stage will be used to prepare battery anodes.

Table 1. The mass ratio of ZnO and graphite for the preparation of ZnO/Graphite

Sample	Mass (g)	
	ZnO powder	Graphite powder
ZnO-C0.5	9	4.5
ZnO-C1	9	9
ZnO-C2	4.5	9
Graphite	0	9

### 2.3. Characterization

XRD (X-Ray Diffraction) data were collected from a diffraction angle ( $2\theta$ ) ranging from  $17^\circ$  to  $70^\circ$  at a rate of  $0.05 \text{ s}^{-1}$ . The crystal structure and size of the sample were determined using XRD data. Furthermore, surface morphology was analyzed using SEM (Scanning Electron Microscopy) (SEM, JEOL JSM-6510LA, Japan) with  $2500\times$  magnification, and the chemical components present in the sample were identified using SEM-EDX (Scanning Electron Microscopy-Energy Dispersive X-Ray) (SEM EDX, JEOL JSM-6510LA, Japan).

### 2.4. Battery Performance Test

Battery assembly testing must be done before performing a battery performance test. At the battery assembly stage, it started by dissolving ZnO/Graphite: AB (Acetylene Black): SBR (Styrene Butadiene Rubber): CMC (Carboxymethyl Cellulose) material in a ratio of 80:10:7:3 with distilled water. The ingredients were mixed using a stirrer to form a paste. The resulting paste was coated with a thin layer on top of Cu foil with a width of  $\pm 5.5 \text{ cm}$  and a thickness of  $\pm 0.2 \text{ cm}$  for each layer, with the final mass of the anode layer was around 4 g. The formed thin layer was then put in the oven until it dried.

The resulting thin anode layer was used to coat the battery components with a separator-anode-separator-cathode arrangement in the battery winding process (Figure 2). Furthermore, the batteries were arranged in a glovebox with an electrolyte solution. The type of electrolyte used was  $\text{LiPF}_6$ . Electrolytes containing  $\text{LiPF}_6$  usually show good conductivity and electrochemical stability and do not promote aluminum corrosion, a material commonly used as a positive electrode current collector [21].

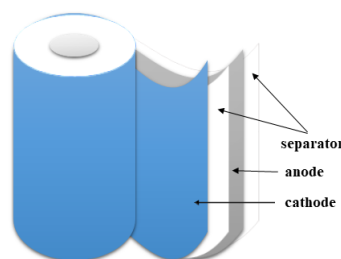


Figure 2. Lithium-ion configuration

In testing battery performance, the test equipment used was an eight-channel battery analyzer (BTS-5V6A, China), which obtained the results of the battery charge-discharge capacity. The performance test is the formation test by running the charge-discharge performance at C/20 and then continuing with the C-rates to see the

capacity's performance when discharge values were set at different stages. C-rate testing was carried out with charge set at 0.5C and discharge rate at 0.1C, 0.2C, 1C, and 2C. The settings 0.1C and 0.2C aimed to determine the slow charge-discharge capacity, 1C for the standard of charge-discharge, and 2C for the fast charge-discharge.

The EIS (Electrochemical Impedance Spectroscopy) (EZstat Pro Nuvant) test analyzed the electrochemical properties of lithium-ion batteries with the frequency range of 0.01 Hz to 10 kHz and the amplitude of 5 mV. The impedance data obtained would be plotted into Nyquist plot using software Origin 2018 version and fit in data using software ZsimDemo 3.2 to acquire the resistance value.

### 3. Results and Discussion

#### 3.1. Crystal Structure and Morphological Analysis

Figure 3 shows the XRD results of ZnO/Graphite composites. XRD results from samples that had been stacked were compared with XRD ZnO pure (commercial) and graphite (commercial) results to obtain a data match. Based on the XRD results, the ZnO-Co.5 revealed the two highest peaks at  $2\theta = 26.8^\circ$  and  $36.59^\circ$  with a crystal size of 18.27 nm. Then, the ZnO-C1 obtained the two highest peaks at  $2\theta = 26.71^\circ$  and  $36.49^\circ$  with a crystal size of 17.31 nm. The ZnO-C2 produced the two highest peaks at  $2\theta = 26.68^\circ$  and  $36.47^\circ$  with a crystal size of 14.75 nm.

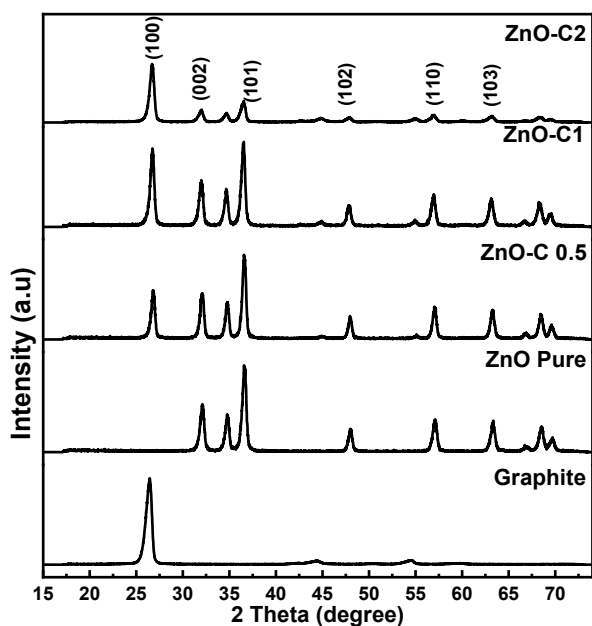


Figure 3. XRD Result

XRD results of ZnO/Graphite composites were compared with JCPDS (Joint Committee on Powder Diffraction Standards) data. In the analysis of the diffraction peaks, all samples of ZnO/Graphite had similar data with JCPDS No. 36-1451, which showed that

ZnO crystals had the first three highest peaks, indicating the diffraction planes of (100), (002), and (101). This peak pattern suggested that the observed ZnO phase had hexagonal Wurtzite [22]. Meanwhile, the results of the graphite analysis had the same data as JCPDS data No. 00-012-0212, which showed that the crystal system was also hexagonal. Furthermore, sample characterization was conducted using SEM to determine the surface morphology of ZnO/Graphite, and the results are shown in Figure 4.

Figure 4 shows the SEM images of ZnO/Graphite and pure graphite. Graphite morphology is in the form of coarse grains with an average diameter of 35.38  $\mu\text{m}$  (Figure 4(a)). The ZnO morphology in Figure 4(b) has a fine structure, even though mainly ZnO is reported to have a spherical and less homogeneous morphology. Figure 4(c-d) shows the morphology of the ZnO/Graphite composite that has been grounded with a mortar for an hour. It is evident that the ZnO particles adhered to the graphite surface and that the produced particles tended to agglomerate into one more significant piece. Based on Figure 4(b-d), it can be said that the mortar process for ZnO and Graphite samples with their mass ratio (Table 1) still requires a longer time, causing uneven agglomeration and less homogeneous morphology. The more homogeneous the ZnO/Graphite composites, the more ZnO crystal growth can be increased, which is helpful for the charge-discharge process.

Table 2. SEM-EDX result of ZnO/Graphite composites

Element	Percentage (%)	
	Mass	Atom
C	77.23±0.56	90.73±0.66
O	7.18±0.45	6.33±0.40
Na	0.72±0.11	0.44±0.07
Zn	9.92±0.46	2.14±0.10
Au	4.95±0.43	0.35±0.03
Total	100.00	100.00

The size of ZnO nanoparticles also has a different effect because the smaller particle size will also cause an increase in surface area, which is directly proportional to the number of reactions that occur so that the reaction results will be better [23]. Incorporating ZnO particles serves as a conductive band and network to allow ZnO particles to combine, significantly reducing the transfer resistance between these particles [24]. This highly affects the intercalation of  $\text{Li}^+$  ions so that it can facilitate the transfer between  $\text{Li}^+$  ions during the battery charge-discharge process.

The elemental composition of the samples was characterized by SEM-EDX, as shown in Table 2. Table 2 demonstrated the presence of C, Zn, and O on the surface of ZnO/Graphite nanoparticles with a ratio of 1:1, along with Au impurities obtained from the samples during SEM preparation.

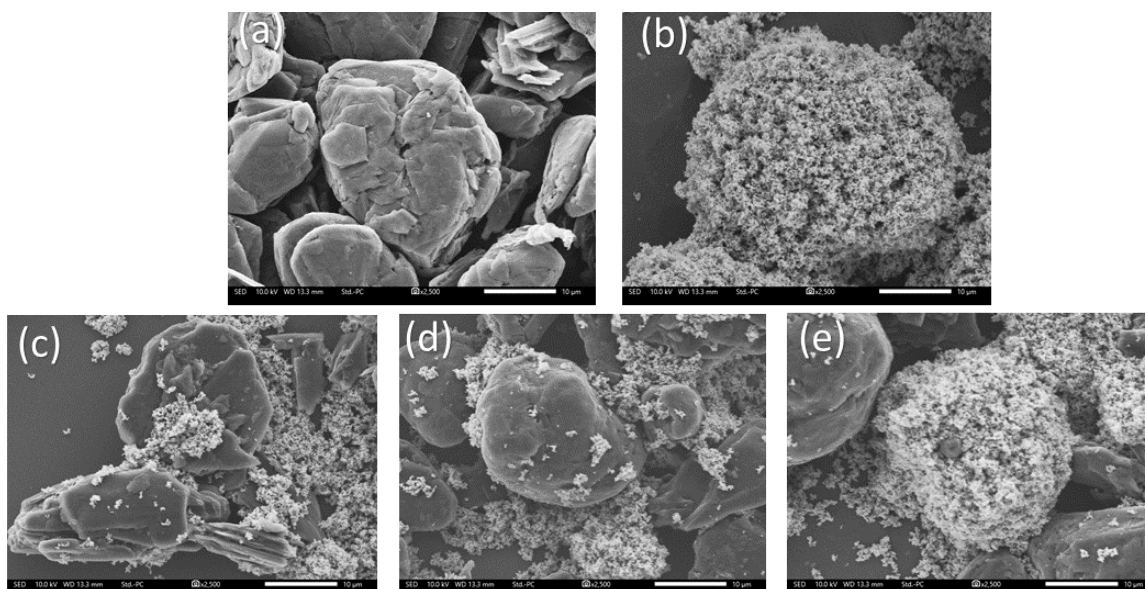


Figure 4. SEM images of (a) graphite, (b) ZnO, (c) ZnO-Co.5, (d) ZnO-C1, (e) ZnO-C2

### 3.2. Impedance Test Results and Charge-Discharge Battery

Figure 5 shows the results of the Nyquist plot data tested by Electrochemical Impedance Spectroscopy (EIS). EIS analysis was performed to investigate the electrodes' charge transfer resistance and ion diffusion performance [25]. The data obtained from the EIS test were in the form of Nyquist plots and linear plots of 4 variations of anode samples. Wang *et al.* [26] said that the Nyquist plot is associated with the charge transfer impedance of the electrode, and the linear plot is associated with the Warburg impedance reflecting the diffusion of solid-state  $\text{Li}^+$  to most of the active materials of the materials used. The Nyquist plot or semi-circle radius directly demonstrates the magnitude of the charge transfer resistance [27].

Table 3. Resistance Value

Sample	$R_1(\text{Ohm})$	$R_2(\text{Ohm})$	Equivalent Circuit
Graphite	27.66	58.32	
ZnO	4.02	5.19	
ZnO-Co.5	0.01	0.36	
ZnO-C1	6.98	57.35	
ZnO-C2	0.21	0.64	

Based on the EIS results (Figure 5 and Table 3), the graphite plot in Figure 5(a) had the most significant resistance, whereas the ZnO-Co.5 plot in Figure 5(c) had the least resistance. This can be seen from the semi-circle that intersects the x-axis. Therefore, the smaller the semicircular plot, the smaller the resistance and the better or greater the conductivity of the battery because the conductivity value is inversely proportional to the resistance value and confirmed by the resistance value obtained from fitting the data through the equivalent circuit using a Nyquist plot (Table 3).

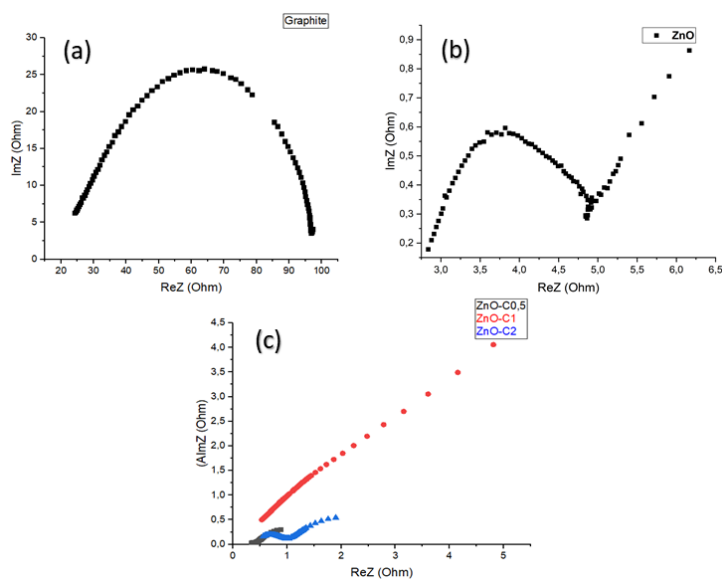


Figure 5. Nyquist plot of (a) Graphite, (b) ZnO, (c) ZnO-Co.5, ZnO-C1, and ZnO-C2

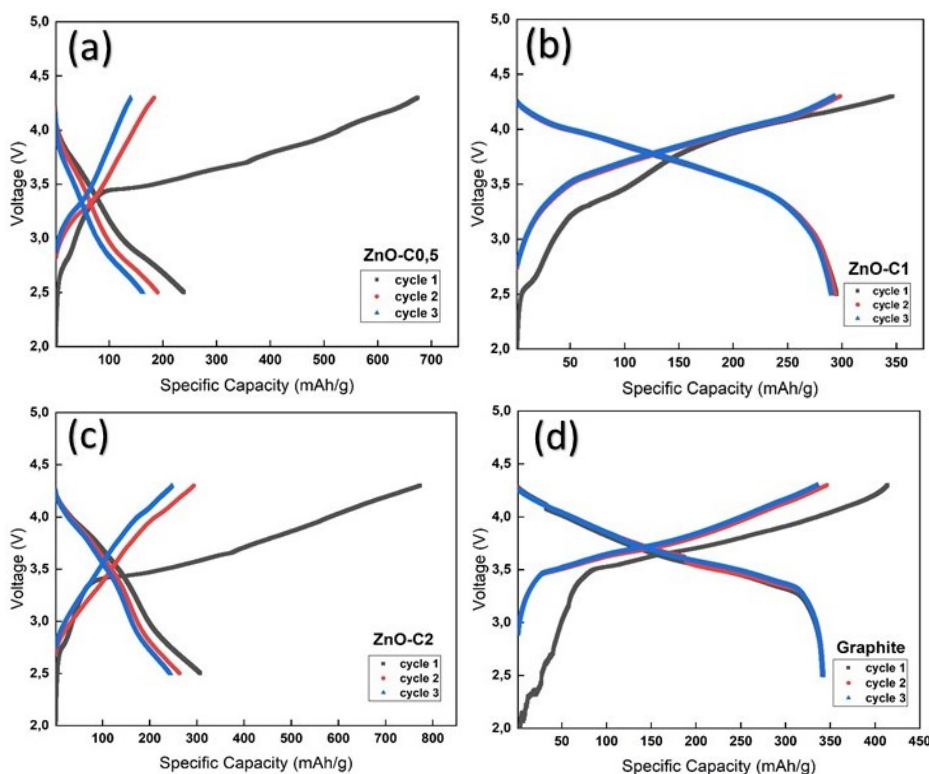


Figure 6. First three charge–discharge of ZnO/Graphite’s lithium–ion batteries (a) ZnO-C0.5, (b) ZnO-C1, (c) ZnO-C2, (d) Graphite

Regarding the results of the morphological analysis of the four anode samples, all zinc oxide graphite composites had a large surface area due to the homogeneity of the mortared ZnO/Graphite. The specific structure of the large ZnO particles can increase the active ingredient’s electrochemical reaction area and reduce the zinc electrode’s resistance and polarization [27]. Zhang *et al.* [28] reported that the priority in determining the performance of battery cells also lies in the surface chemistry aspect, which produces good surface contact to ensure the intercalation and deintercalation processes run well during the battery charge–discharge process.

Figure 6 displays graphs of the charge and discharge process for the four anode modifications performed with the first three cycles, which constitute the formation phase, to determine the precise lithium–ion battery capacity. This is attributed to the fact that the battery capacity depends on the active material type and the electrochemical reaction rate during charging and discharging. The broader surface contact between the active materials will also increase the battery capacity. The amount of lithium–ions that may be transported to the anode increases with the electric current generated during discharging [29].

Table 4. Coulombic efficiency at the first three cycles

Cycle Number	Graphite	ZnO-C0.5	ZnO-C1	ZnO-C2
Cycle 1	76%	23%	79%	33%
Cycle 2	95%	73%	96%	81%
Cycle 3	95%	81%	97%	89%

As seen from all variations of the battery anode samples, the four variations have specific capacity values in the range of 150–350 mAh/g. Yang *et al.* [24] added that

a full battery of ZnO/Graphite shows a capacity of around 280–400 mAh/g. and is a superior speed capability. In Figure 6, all ZnO/Graphite batteries have a specific discharge capacity stabilizing in the second cycle. This is because, during the first charge–discharge process, the lithium–ion battery undergoes surface electrochemical interphase (SEI), which is electrolyte decomposition that produces a high irreversible capacity during the first discharge process and starts to stabilize in the second and subsequent cycles. The active material of SEI is derived from the positive electrode material and is responsible for the irreversible capacity, which suffers significant losses in the first cycle of most Li-ion batteries [30].

This has been demonstrated by the calculated Columbia efficiency (CE) values in Table 4. CE is the ratio of discharge capacity value divided by the charge capacity value [31]. This suggests that ZnO can be considered a material that can improve the charge transfer efficiency and electron transfer rate of the electrodes, which will help enhance stability and good capacity during battery discharge.

Figure 7 shows the performance value of the specific discharge capacity rate of the battery (the C-rate). The C-rate testing was carried out under three charge–discharge cycles, with charge setting at 0.5C and discharge rate at 0.1, 0.2, 1, and 2C. ZnO-C1 anode and graphite have the most stable specific discharge capacity. As can be observed, the particular capacity value did not significantly decrease even when it was configured with different C-rates. Figure 7 shows that the higher the C-rate, the smaller the specific capacity for discharging the battery.

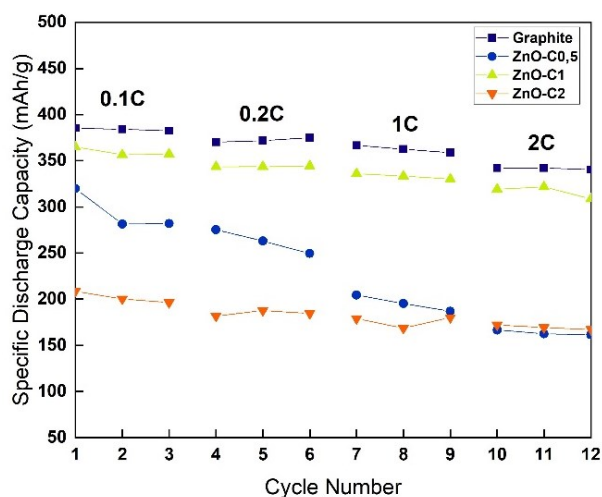


Figure 7. Rate ability of ZnO/Graphite's lithium-ion battery

The specific discharge capacity decreases towards the next cycle, and the capacity decrease during the discharging and charging processes due to the volume expansion of the ZnO particles. The results showed that morphological control could overcome problems using ZnO material as an anode of lithium-ion batteries, such as volume expansion and battery shutdown in just a few cycles [22]. This phenomenon can also be attributed to the enlarged interplanar distance and reduced activation barrier for using Li<sup>+</sup> with the active materials [32]. Zhang *et al.* [28] also added that the charge-discharge capacity for the second cycle, both ZnO and graphene, showed good electrode stability and consistent cycle performance.

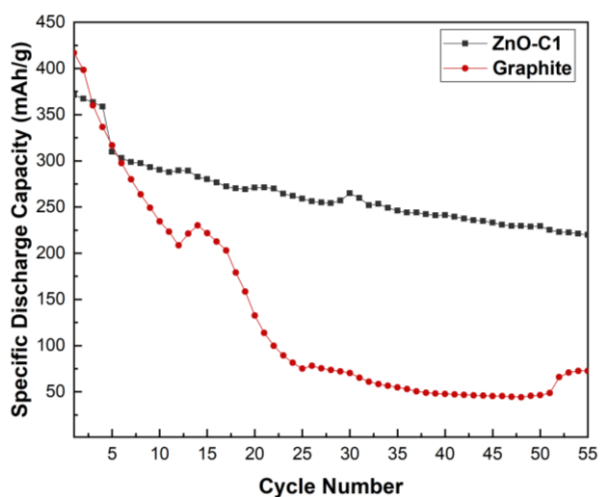


Figure 8. Cycle performance of ZnO/Graphite's lithium-ion battery

Figure 8 shows ZnO/Graphite stability after charge-discharge with several cycles. It can be seen that the ZnO/Graphite anode displayed a better cycle performance, which resulted in a constant significant capacity decrease from the initial cycle to cycle 55<sup>th</sup> with a specific capacity discharge range of 219.72–371.27 mAh/g and decreased value of 40%. Compared to the graphite sample, the specific capacity discharge ranged from 72.62 to 416.9 mAh/g, with a decrease value of more than 80%. This result is in line with the research conducted by Wang

*et al.* [33], which reported that a stable cycle was achieved after several cycles. According to the EIS results, the ZnO/Graphite anode also showed a lower charge transfer resistance than the commercial graphite electrode, meaning that the ZnO/Graphite anode can produce better electrode reaction kinetic characteristics (charge transfer and polarization). It also could be ascribed to better electron availability and possibly Li<sup>+</sup>. A better type of crystal is also a fast pathway for mass transport and electron transfer, increasing Li's storage capacity [34].

All variations of ZnO/Graphite anodes had sufficient specific capacity rate stability, which can be concluded that ZnO/Graphite may be considered a continuous anode material for lithium-ion batteries. Apart from the high specific capacity and stability of ZnO, the active material ZnO contained in the anode can also act as a continuous anode material because it has a stable structure [29]. However, some considerations are still required in producing anode material from ZnO/Graphite, such as the homogeneity of the sample. The homogeneity of the samples must be taken into account since the shape of the sample has a significant influence on its chemical properties for the cycle performance of the charge-discharge process for lithium-ion batteries.

#### 4. Conclusion

ZnO/Graphite composites were prepared using a solid-state method with different ratio mass of graphite and ZnO. XRD results showed the ZnO/Graphite composites had crystal peaks that matched the JCPDS database with an agglomerate morphology where the ZnO adhered to the graphite according to the SEM images. The characterization led to the results of the battery performance testing data. As a result, the ZnO-C1 for the lithium-ion battery was fabricated and had a specific value of stable capacity at 219.72–371.27 mAh/g with a decreased value of 40%. This result showed that the ZnO-C1 had better stability than pure graphite. The EIS impedance graph confirmed that the ZnO-C1 had a lower resistance value than graphite, allowing it to store more electrons. Therefore, the ZnO-C1 can be a candidate for active material additives at the lithium-ion battery anode.

#### References

- [1] Tiancai Jiang, Fanxing Bu, Xiaoxiang Feng, Imran Shakir, Guolin Hao, Yuxi Xu, Porous Fe<sub>2</sub>O<sub>3</sub> nanoframeworks encapsulated within three-dimensional graphene as high-performance flexible anode for lithium-ion battery, *ACS Nano*, 11, 5, (2017), 5140–5147 <https://doi.org/10.1021/acsnano.7b02198>
- [2] Hendri Widiyandari, Atika Nadya Sukmawati, Heri Sutanto, Cornelius Yudha, Agus Purwanto, Synthesis of LiNi<sub>0.8</sub>Mn<sub>0.1</sub>Co<sub>0.1</sub>O<sub>2</sub> cathode material by hydrothermal method for high energy density lithium ion battery, *Journal of Physics: Conference Series*, 2019 <https://doi.org/10.1088/1742-6596/1153/1/012074>
- [3] Guanglei Wu, Zirui Jia, Yonghong Cheng, Hongxia Zhang, Xinfeng Zhou, Hongjing Wu, Easy synthesis of multi-shelled ZnO hollow spheres and their conversion into hedgehog-like ZnO hollow spheres

- with superior rate performance for lithium ion batteries, *Applied Surface Science*, 464, (2019), 472–478 <https://doi.org/10.1016/j.apsusc.2018.09.115>
- [4] Changlei Xiao, Shichao Zhang, Shengbin Wang, Yalan Xing, Ruoxu Lin, Xin Wei, Wenxu Wang, ZnO nanoparticles encapsulated in a 3D hierarchical carbon framework as anode for lithium ion battery, *Electrochimica Acta*, 189, (2016), 245–251 <https://doi.org/10.1016/j.electacta.2015.11.045>
- [5] Minjie Shi, Tianhao Wu, Xuefeng Song, Jing Liu, Liping Zhao, Peng Zhang, Lian Gao, Active Fe<sub>2</sub>O<sub>3</sub> nanoparticles encapsulated in porous g-C<sub>3</sub>N<sub>4</sub>/graphene sandwich-type nanosheets as a superior anode for high-performance lithium-ion batteries, *Journal of Materials Chemistry A*, 4, 27, (2016), 10666–10672 <https://doi.org/10.1039/C6TA03533G>
- [6] Yimo Xiang, Zhigao Yang, Shengping Wang, Md. Shahriar A. Hossain, Jingxian Yu, Nanjundan Ashok Kumar, Yusuke Yamauchi, Pseudocapacitive behavior of the Fe<sub>2</sub>O<sub>3</sub> anode and its contribution to high reversible capacity in lithium ion batteries, *Nanoscale*, 10, 37, (2018), 18010–18018 <https://doi.org/10.1039/C8NR04871A>
- [7] Huan Liu, Shao-hua Luo, Dong-bei Hu, Xin Liu, Qing Wang, Zhi-yuan Wang, Ying-ling Wang, Long-jiao Chang, Yan-guo Liu, Ting-Feng Yi, Design and synthesis of carbon-coated  $\alpha$ -Fe<sub>2</sub>O<sub>3</sub>@Fe<sub>3</sub>O<sub>4</sub> heterostructured as anode materials for lithium ion batteries, *Applied Surface Science*, 495, 143590, (2019), 1–8 <https://doi.org/10.1016/j.apsusc.2019.143590>
- [8] Subhalaxmi Mohapatra, Shantikumar V. Nair, Dhamodaran Santhanagopalan, Alok Kumar Rai, Nanoplate and mulberry-like porous shape of CuO as anode materials for secondary lithium ion battery, *Electrochimica Acta*, 206, (2016), 217–225 <https://doi.org/10.1016/j.electacta.2016.04.116>
- [9] P. Subalakshmi, A. Sivashanmugam, CuO nano hexagons, an efficient energy storage material for Li-ion battery application, *Journal of Alloys and Compounds*, 690, (2017), 523–531 <https://doi.org/10.1016/j.jallcom.2016.08.157>
- [10] Wei Yuan, Zhiqiang Qiu, Yu Chen, Bote Zhao, Meilin Liu, Yong Tang, A binder-free composite anode composed of CuO nanosheets and multi-wall carbon nanotubes for high-performance lithium-ion batteries, *Electrochimica Acta*, 267, (2018), 150–160 <https://doi.org/10.1016/j.electacta.2018.02.081>
- [11] Ping Wang, Xiao-Xia Gou, Sen Xin, Fei-Fei Cao, Facile synthesis of CuO nanochains as high-rate anode materials for lithium-ion batteries, *New Journal of Chemistry*, 43, 17, (2019), 6535–6539 <https://doi.org/10.1039/C9NJ01015G>
- [12] Chungo Kim, Jin Wook Kim, Hyunhong Kim, Dong Hyeon Kim, Changhoon Choi, Yoon Seok Jung, Jongnam Park, Graphene oxide assisted synthesis of self-assembled zinc oxide for lithium-ion battery anode, *Chemistry of Materials*, 28, 23, (2016), 8498–8503 <https://doi.org/10.1021/acs.chemmater.5b03587>
- [13] Xin Wang, Lanyan Huang, Yan Zhao, Yongguang Zhang, Guofu Zhou, Synthesis of mesoporous ZnO nanosheets via facile solvothermal method as the anode materials for lithium-ion batteries, *Nanoscale Research Letters*, 11, 37, (2016), 1–6 <https://doi.org/10.1186/s11671-016-1244-9>
- [14] Denghu Wei, Zhijun Xu, Jie Wang, Yuanwei Sun, Suyuan Zeng, Wenzhi Li, Xiaona Li, A one-pot thermal decomposition of C<sub>4</sub>H<sub>4</sub>ZnO<sub>6</sub> to ZnO@carbon composite for lithium storage, *Journal of Alloys and Compounds*, 714, (2017), 13–19 <https://doi.org/10.1016/j.jallcom.2017.04.214>
- [15] Ludi Shi, Dongzhi Li, Jiali Yu, Han-Ming Zhang, Shahid Ullah, Bo Yang, Cuihua Li, Caizhen Zhu, Jian Xu, Rational design of hierarchical ZnO@Carbon nanoflower for high performance lithium ion battery anodes, *Journal of Power Sources*, 387, (2018), 64–71 <https://doi.org/10.1016/j.jpowsour.2018.03.047>
- [16] Tiezhong Liu, Yayun Guo, Shuang Hou, Wenpei Fu, Juan Li, Lingyu Meng, Chen Mei, Lingzhi Zhao, Constructing hierarchical ZnO@C composites using discarded Sprite and Fanta drinks for enhanced lithium storage, *Applied Surface Science*, 541, 148495, (2021), 1–10 <https://doi.org/10.1016/j.apsusc.2020.148495>
- [17] M. Laurenti, N. Garino, S. Porro, M. Fontana, C. Gerbaldi, Zinc oxide nanostructures by chemical vapour deposition as anodes for Li-ion batteries, *Journal of Alloys and Compounds*, 640, (2015), 321–326 <https://doi.org/10.1016/j.jallcom.2015.03.222>
- [18] Ruitian Guo, Yan Wang, Xiaojian Shan, Yongkang Han, Zhang Cao, Honghe Zheng, A novel itaconic acid-graphite composite anode for enhanced lithium storage in lithium ion batteries, *Carbon*, 152, (2019), 671–679 <https://doi.org/10.1016/j.carbon.2019.06.065>
- [19] Yoon Ji Jo, Jong Dae Lee, Effect of petroleum pitch coating on electrochemical performance of graphite as anode materials, *Korean Journal of Chemical Engineering*, 36, 10, (2019), 1724–1731 <https://doi.org/10.1007/s11814-019-0354-3>
- [20] Aijia Wei, Wen Li, Xue Bai, Lihui Zhang, Zhenfa Liu, Yanji Wang, A facile one-step solid-state synthesis of a Li<sub>4</sub>Ti<sub>5</sub>O<sub>12</sub>/graphene composite as an anode material for high-power lithium-ion batteries, *Solid State Ionics*, 329, (2019), 110–118 <https://doi.org/10.1016/j.ssi.2018.11.023>
- [21] Larry J. Krause, William Lamanna, John Summerfield, Mark Engle, Gary Korba, Robert Loch, Radoslav Atanasoski, Corrosion of aluminum at high voltages in non-aqueous electrolytes containing perfluoroalkylsulfonfyl imides; new lithium salts for lithium-ion cells, *Journal of Power Sources*, 68, 2, (1997), 320–325 [https://doi.org/10.1016/S0378-7753\(97\)02517-2](https://doi.org/10.1016/S0378-7753(97)02517-2)
- [22] Hongbo Wang, Qinmin Pan, Yuexiang Cheng, Jianwei Zhao, Geping Yin, Evaluation of ZnO nanorod arrays with dandelion-like morphology as negative electrodes for lithium-ion batteries, *Electrochimica Acta*, 54, 10, (2009), 2851–2855 <https://doi.org/10.1016/j.electacta.2008.11.019>
- [23] Tety Sudiarti, Neng Hani Handayani, Yusuf Rohmatulloh, Silmi Rahma Amelia, Ravli Maulana Yusuf, Atthar Luqman Ivansyah, Facile Synthesis of ZnO Nanoparticles for the Photodegradation of Rhodamine-B, *Jurnal Kimia Sains dan Aplikasi*, 24, 6, (2021), 185–191 <https://doi.org/10.14710/jksa.24.6.185-191>

- [24] Xiaofei Yang, Jingyi Qiu, Meng Liu, Hai Ming, Huimin Zhang, Meng Li, Songtong Zhang, Tingting Zhang, A surface multiple effect on the ZnO anode induced by graphene for a high energy lithium-ion full battery, *Journal of Alloys and Compounds*, 824, 153945, (2020), 1-12  
<https://doi.org/10.1016/j.jallcom.2020.153945>
- [25] Muslum Demir, Sushil Kumar Saraswat, Ram B. Gupta, Hierarchical nitrogen-doped porous carbon derived from lecithin for high-performance supercapacitors, *RSC Advances*, 7, 67, (2017), 42430-42442 <https://doi.org/10.1039/C7RA07984B>
- [26] Limin Wang, Zhanhong Yang, Xi Chen, Haigang Qin, Peng Yan, Formation of porous ZnO microspheres and its application as anode material with superior cycle stability in zinc-nickel secondary batteries, *Journal of Power Sources*, 396, (2018), 615-620  
<https://doi.org/10.1016/j.jpowsour.2018.06.031>
- [27] Guanghui Yuan, Jiming Xiang, Huafeng Jin, Lizhou Wu, Yanzi Jin, Yan Zhao, Anchoring ZnO nanoparticles in nitrogen-doped graphene sheets as a high-performance anode material for lithium-ion batteries, *Materials*, 11, 1, (2018), 96  
<https://doi.org/10.3390/ma11010096>
- [28] Junfan Zhang, Taizhe Tan, Yan Zhao, Ning Liu, Preparation of ZnO nanorods/graphene composite anodes for high-performance lithium-ion batteries, *Nanomaterials*, 8, 12, (2018), 1-9  
<https://doi.org/10.3390/nano8120966>
- [29] Yoyok Dwi Setyo Pambudi, Rudy Setiabudy, Akhmad Herman Yuwono, Evvy Kartini, Joong Kee Lee, Chairul Hudaya, Effects of annealing temperature on the electrochemical characteristics of ZnO microrods as anode materials of lithium-ion battery using chemical bath deposition, *Ionics*, 25, 2, (2019), 457-466  
<https://doi.org/10.1007/s11581-018-2723-z>
- [30] R. Hausbrand, G. Cherkashinin, H. Ehrenberg, M. Gröting, K. Albe, C. Hess, W. Jaegermann, Fundamental degradation mechanisms of layered oxide Li-ion battery cathode materials: Methodology, insights and novel approaches, *Materials Science and Engineering: B*, 192, (2015), 3-25 <https://doi.org/10.1016/j.mseb.2014.11.014>
- [31] Chengcheng Fang, Jinxing Li, Minghao Zhang, Yihui Zhang, Fan Yang, Jungwoo Z. Lee, Min-Han Lee, Judith Alvarado, Marshall A. Schroeder, Yangyuchen Yang, Quantifying inactive lithium in lithium metal batteries, *Nature*, 572, 7770, (2019), 511-515  
<https://doi.org/10.1038/s41586-019-1481-z>
- [32] Wei Pan, Wenjie Peng, Huajun Guo, Jiexi Wang, Zhixing Wang, Hangkong Li, Kaimin Shih, Effect of molybdenum substitution on electrochemical performance of  $\text{Li}[\text{Li}_{0.2}\text{Mn}_{0.54}\text{Co}_{0.13}\text{Ni}_{0.13}]\text{O}_2$  cathode material, *Ceramics International*, 43, 17, (2017), 14836-14841  
<https://doi.org/10.1016/j.ceramint.2017.07.232>
- [33] Leying Wang, Xiayu Zhu, Yuepeng Guan, Jinliang Zhang, Fei Ai, Wenfeng Zhang, Yu Xiang, Srinivasapriyan Vijayan, Guodong Li, Yaqin Huang, ZnO/carbon framework derived from metal-organic frameworks as a stable host for lithium metal anodes, *Energy Storage Materials*, 11, (2018), 191-196  
<https://doi.org/10.1016/j.ensm.2017.10.016>
- [34] Wenhui Zhang, Lijuan Du, Zongren Chen, Juan Hong, Lu Yue, ZnO nanocrystals as anode electrodes for lithium-ion batteries, *Journal of Nanomaterials*, 2016, 8056302, (2016), 1-7  
<https://doi.org/10.1155/2016/8056302>